Title: Crystal structures of EfeB and EfeO in a bacterial siderophore-independent iron transport system

Authors: Sakiko Nakatsuji[a, 1], Kenji Okumura[a, 1], Ryuichi Takase[a], Daisuke Watanabe[a], Bunzo Mikami[b], and Wataru Hashimoto[a, *]

[a]Laboratory of Basic and Applied Molecular Biotechnology, Division of Food Science and Biotechnology, Graduate School of Agriculture, Kyoto University, Uji, Kyoto 611-0011, Japan.

[b]Laboratory of Metabolic Sciences of Forest Plants and Microorganisms, Research Institute for Sustainable Humanosphere, Kyoto University, Uji, Kyoto 611-0011, Japan

[1]Sakiko Nakatsuji and Kenji Okumura contributed equally to this work.

[*]Corresponding author. E-mail address: hashimoto.wataru.8c@kyoto-u.ac.jp (W. Hashimoto)

Abstract

EfeUOB is a siderophore-independent iron uptake mechanism in bacteria. EfeU, EfeO, and EfeB are a permease, an iron-binding or electron-transfer protein, and a peroxidase, respectively. A Gram-negative bacterium, *Sphingomonas* sp. strain A1, encodes EfeU, EfeO, EfeB together with alginate-binding protein Algp7, a truncated EfeO-like protein ($EfeO_{II}$), in the genome. The typical EfeO ($EfeO_I$) consists of N-terminal cupredoxin and C-terminal M75 peptidase domains. Here, we detail the structure and function of bacterial EfeB and EfeO. Crystal structures of strain A1 EfeB and *Escherichia coli* $EfeO_I$ were determined at 2.30 Å and 1.85 Å resolutions, respectively. A molecule of heme involved in oxidase activity was bound to the C-terminal Dyp peroxidase domain of EfeB. Two domains of $EfeO_I$ were connected by a short loop, and a zinc ion was bound to four residues, Glu156, Glu159, Asp173, and Glu255, in the C-terminal M75 peptidase domain. These residues formed tetrahedron geometry suitable for metal binding and are well conserved among various EfeO proteins including Algp7 ($EfeO_{II}$), although the metal-

binding site (HxxE) is proposed in the C-terminal M75 peptidase domain. This is the first report on structure of a typical EfeO with two domains, postulating a novel metal-binding motif "ExxE-//-D-//-E" in the EfeO C-terminal M75 peptidase domain.

Keywords: EfeB, EfeO, iron transport, X-ray crystallography

1. Introduction

Iron is essential for various enzymatic reactions, protein stabilization, and signal transduction *in vivo*. A typical mechanism used by microorganisms to acquire iron from the external environment is the use of siderophores, which are metal chelators. Microorganisms secrete siderophores, which form Fe^{3+}–siderophore complexes extracellularly and solubilize Fe^{3+}, and subsequently acquire iron by importing the Fe^{3+}–siderophore complex into the cell [1]. Another mechanism for iron import is the Efe system [2]. The Efe system functions

1 independently of siderophores and consists of three proteins, namely, EfeU, EfeO, and EfeB,
2 and it was first identified in *Escherichia coli* strain O157:H7 [3]. The expression of Efe proteins
3 is induced by low pH or iron concentration. EfeU probably functions as a permease and
4 localizes in the inner membrane. The periplasmic protein EfeB containing heme shows
5 peroxidase activity to oxidize Fe^{2+} to Fe^{3+} [4]. EfeO shows iron-binding or electron-transfer
6 activity and is located in the periplasm. EfeO has variations in its domain topology [5]. A typical
7 EfeO is classified as $EfeO_I$, composed of an N-terminal cupredoxin and C-terminal M75
8 peptidase domains. The cupredoxin is a copper-binding protein involved in stabilizing Cu^{2+}
9 during copper uptake [6], and the M75 peptidase binds zinc ions [7]. The cupredoxin and M75
10 peptidase domains in EfeO contain two and one metal-binding motifs, respectively [5]. Distinct
11 from $EfeO_I$, $EfeO_{II}$, possessing only M75 peptidase domain, forms another group of EfeO.
12 Nevertheless the tertiary structure of $EfeO_{II}$ is available, that of $EfeO_I$ remains to be clarified,
13 obstructing understanding of molecular mechanism of Efe system.

The Gram-negative and alginate-assimilating *Sphingomonas* sp. strain A1 possesses an Efe system consisting of EfeUO$_{I}$B and one additional EfeO$_{II}$ protein, Algp7 (SPH726) (Fig. 1A). Another EfeO$_{I}$ protein, SPH728, has a conserved N-terminal cupredoxin and C-terminal M75 peptidase domains. Algp7 (EfeO$_{II}$) exhibits a high alginate-binding ability with a dissociation constant (K_d value) of 3.6×10^{-8} M and functions to concentrate alginate on the cell surface [8-9]. Algp7 (EfeO$_{II}$) binds Cu^{2+}, Fe^{2+}, and Zn^{2+} as well as alginate [10]. Strain A1 incorporates alginate as a polysaccharide into the cytoplasm through a cell surface pit containing Algp7 (EfeO$_{II}$) and an ATP-binding cassette transporter [9].

Alginate polysaccharide constituents are broadly classified into three types: polymannuronic acid blocks (M-blocks), polyguluronic acid blocks (G-blocks), and random blocks. Various metals, including iron, are chelated into alginate G-blocks [10]. Therefore, strain A1 probably acquires metals by binding extracellular alginate with Algp7 (EfeO$_{II}$), which binds both alginate and metals. The elucidation of the mechanism of metal import using alginate

in strain A1 should provide important insights into alginate-dependent metal physiology in bacteria. Furthermore, bacterial metal import machinery can be applied to bioremediation and recovery of useful metals, including rare earth elements. This article describes the structure and function of the Efe system component proteins, namely, EfeB and EfeO.

2. Materials and methods

2.1. Reagents

General reagents of special grade were purchased from Fujifilm Wako Pure Chemicals and Nacalai Tesque. Samarium (III) sulfate octahydrate was obtained from Sigma-Aldrich.

2.2. Strains and media

E. coli strains BL21(DE3), Rosetta-gami 2(DE3), and MG1655 were used in this study. Luria Bertani (LB) medium (1% tryptone, 0.5% yeast extract, and 1% NaCl) was used to culture

the *E. coli* strains.

2.3. Protein expression and purification

(i) EfeB

Recombinant EfeB was expressed in *E. coli* strain Rosetta-gami 2(DE3) harboring the plasmid pET21b-EfeB that encoded EfeB with a hexahistidine tag at the C-terminus. The EfeB gene was amplified from the strain A1 genome by PCR using synthetic oligo DNA primers (forward: 5′-GGCATATGGATGAGATCGAAAACGGCAAGG-3′, reverse: 5′-CCGCCGCCGCGCGCGCACTGGCGTCCA-3′). The resultant fragment was ligated with pET21b and treated with restriction enzymes NdeI and NotI. The transformed cells with pET21b-EfeB were cultured in LB medium containing 0.1 mg/mL sodium ampicillin at 37°C and 100 spm for 3 h. At the exponential growth phase, isopropyl β-D-1-thiogalactopyranoside (IPTG) was added to the medium to a final concentration of 0.1 mM, and then, the culture was

incubated for another 44 h at 16°C. The culture was centrifuged (14,450 × g, 4°C, 10 min), the supernatant was removed, and the pellet was suspended in 20 mM Tris-HCl (pH 7.5). The suspension was treated with an ultrasonic disrupter (Insonator Model 201M, Kubota) at 9 kHz for 20 min, and cell extracts were obtained by centrifugation (18,000 × g, 4°C, 20 min). EfeB was purified from the cell extracts using TALON metal affinity resin (bed volume, 10 mL; Takara Bio), and Hi Load 16/60 Superdex 75 pg column (1.6 × 10 cm; GE Healthcare). Purified EfeB was then dialyzed using 20 mM Tris-HCl (pH 7.5). All purifications were conducted at 4°C. The concentration of purified EfeB was calculated by measuring Abs_{280} with an absorption coefficient for EfeB of 34,045 $M^{-1}cm^{-1}$.

(ii) Algp7 ($EfeO_{II}$)

E. coli strain BL21(DE3) was transformed with the expression plasmid pET44a-Algp7 [8]. The plasmid encoded the Algp7 ($EfeO_{II}$) fusion protein that had a hexahistidine tag on the C-terminus and a NusA tag on the N-terminus. Expression and purification of Algp7 ($EfeO_{II}$) were

conducted as described previously [9]. The concentration of purified Algp7 ($EfeO_{II}$) was determined by measuring the absorbance at a wavelength of 280 nm (Abs_{280}) with an absorbance coefficient for Algp7 ($EfeO_{II}$) of 17,420 $M^{-1}cm^{-1}$.

(iii) $EfeO_I$

The plasmid pET21b-EfeO encoding *E. coli* EfeO without signal sequence was constructed in the same way with EfeB except for the gene and primers. The $EfeO_I$ gene was amplified from the strain MG1655 genome by PCR using DNA primers (forward: 5′-AAGGAGATATACATATGGCTGATGTGCCGCAGGTCAAAGTGACC-3′, reverse: 5′-GGTGGTGGTGCTCGAGATCCAGTCCCAGCACACCGCGAAGTTG-3′). *E. coli* strain BL21(DE3) cells were transformed with the resultant plasmid and cultured in 13.5 L of LB medium containing 0.1 mg/mL sodium ampicillin at 37°C and 108 spm. At the exponential growth phase, IPTG was added at a final concentration of 0.4 mM followed by further incubation at 16ºC for 48 h. Cell collection and disruption were conducted in the same way

with EfeB followed by purification using TALON metal affinity resin (bed volume; 30 mL), HiLoad 26/10 Q-Sepharose HP column (2.6 × 10 cm), HiLoad 16/10 Phenyl Sepharose column (1.6 × 10 cm; GE healthcare), HiLoad 16/60 Superdex 200 pg column (1.6 × 60 cm; GE healthcare), and Mono Q HR 5/5 column (0.5 × 5 cm; GE healthcare).

2.4. Crystallization and structure determination

Each of purified EfeB, Algp7 ($EfeO_{II}$), and $EfeO_I$ was crystallized. Crystallization was performed in a 96-well plate using the sitting-drop vapor diffusion equilibrium method. One microliter of 10 mg/mL EfeB solution was mixed with the same amount of crystallization liquid [15% polyethylene glycol 400, 100 mM sodium acetate (pH 4.6), and 100 mM $CaCl_2$]. One microliter of crystallization liquid [12.5% polyethylene glycol 8,000, 100 mM sodium citrate (pH 3.9), and 200 mM NaCl] was added to 1 μL of 8 mg/mL Algp7 ($EfeO_{II}$) solution. One microliter of 20 mg/mL $EfeO_I$ solution was mixed with the same amount of crystallization

liquid [20% polyethylene glycol 4,000, 160 mM ammonium sulfate, 80 mM sodium acetate (pH 4.6), and 20% glycerol].

Algp7 ($EfeO_{II}$) crystals were soaked in the crystallization parent liquid with 5 mM $Sm_2(SO_4)_3$ for 15 min. The crystals were frozen in liquid nitrogen and then were analyzed at the BL38B1 beamline at SPring-8 (Hyogo, Japan). Similarly, EfeB and $EfeO_I$ crystals were soaked in the crystallization liquid with 20% ethylene glycol and frozen with liquid nitrogen, and then were analyzed at the BL26B1 and BL38B1 beamlines, respectively, at SPring-8.

Each frozen crystal was irradiated with X-rays at a wavelength of 1.00 Å. The diffraction data were collected using detector MX225-HS CCD (Rayonix) at BL26B1 or PILATUS3X 2M (Dectris) at BL38B1 and then processed by *HKL2000* [11] or *XDS* [12]. The software *Molrep* [13] included in the CCP4interface (CCP4i) package was used for molecular replacement. Structural refinement was performed using *Phenix.refine* [14] and *Refmac5* [15], the model was manually modified using *WinCoot* [16], and the figure was generated using *PyMol* [17]. The

structure of cupredoxin domain in $EfeO_I$ was constructed manually referring to the electron density map using *WinCoot* because of the lack of the coordinate model in the Protein Data Bank (PDB) database. The atomic coordinates and structure factors (PDB ID: 6JBN for EfeB, 6JBO for Algp7 ($EfeO_{II}$), and 7WGU for $EfeO_I$) were deposited in PDB, Research Collaboratory for Structural Bioinformatics, Rutgers University, New Brunswick, NJ (http://www.rcsb.org/).

2.5. Inductively coupled plasma-mass spectrometry (ICP-MS) analysis

The purified $EfeO_I$ in 20 mM Tris-HCl (pH 7.5) was concentrated using VIVA SPIN 500 (Sartorius) to a final concentration of 48.7 mM. The solution (900 μL) was subjected to the ICP-MS analysis. Data collection and analysis was conducted by Tokai Technology Center (Aichi, Japan).

2.6. Differential scanning fluorimetry (DSF)

Algp7 ($EfeO_{II}$) binding affinity for a rare earth element (Sm^{3+}) was evaluated using DSF in the presence or absence of the element as described previously [18].

2.7. Measuring EfeB peroxidase activity

Nitrogen gas was injected into the glove box S-GBC type (Samplatec) to create an anaerobic environment. In the glove box, 20 μM EfeB was added to the reaction solution containing 3 mM $FeSO_4 \cdot 7H_2O$ and 1 mM H_2O_2. The concentration of Fe^{2+} in the reaction solution was determined by the nitroso-PSAP method using a metallo assay iron measurement kit (Funakoshi). Nitroso-PSAP forms a complex with Fe^{2+} and exhibits coloration with a peak at a wavelength of 750 nm [19]. Fifteen microliters of a 10-fold diluted sample was mixed with 160 μL of ultrapure water or 30% guanidine hydrochloride as a surfactant and 160 μL of 1% sodium ascorbate as the reducing agent, followed by incubation for 10 min. Seventy-five microliters of

0.1% nitroso-PSAP was added to the solution and incubated for 5 min. The peroxidase activity of EfeB was determined by measuring the absorbance of the solution at a wavelength of 750 nm to determine the concentration of residual Fe^{2+}.

3. Results and discussion

3.1. EfeB includes heme in the crystal structure

Strain A1 EfeB was crystallized, and its tertiary structure was determined by X-ray crystallography. The statistics of X-ray diffraction and structure refinement data are shown in Table S1. His231 and Ala269 were the anomalous regions in the Ramachandran plot for chains A and B, respectively. The crystal structure of EfeB from *E. coli* strain O157:H7 has been previously reported (PDB ID: 3O72) [4]. EfeB from *E. coli* and from strain A1 showed high sequence similarity (identity: 60%), and both had a Dyp peroxidase domain on the C-terminus. The tertiary structure of EfeB from strain A1 was, therefore, similar to that of EfeB from *E. coli*.

Strain A1 EfeB contained 14 α-helices and 13 β-strands, and the antiparallel β-sheet consisting of four β-strands was sandwiched by α-helices (Fig. 1B). A heme molecule was bound to the C-terminal Dyp peroxidase domain (Fig. 1C).

3.2. Oxidation activity of EfeB against Fe^{2+}

Because nitroso-PSAP is inactive in the presence of Fe^{3+}, Fe^{2+} concentration is measured in the absence of a reducing agent. If a reducing agent is present, total concentrations of Fe^{3+} and Fe^{2+} are measured to account for the fact that Fe^{3+} is reduced to Fe^{2+} by the reducing reagent. In the presence of EfeB but in the absence of a reducing agent, the Fe^{2+} concentration decreased significantly after 10 min of reaction time (Fig. 1D). Conversely, in the presence of Algp7 ($EfeO_{II}$) or in the negative control, there was no decrease of the Fe^{2+} concentration without the reducing agent (Fig. 1D). These results indicated that EfeB exhibits peroxidase activity and oxidizes Fe^{2+} to Fe^{3+}. EfeB peroxidase activity also occurred in the absence of H_2O_2, suggesting

that EfeB oxidized using dissolved oxygen in the reaction solution (Fig. 1D).

3.3. Rare earth element-binding ability of Algp7 ($EfeO_{II}$)

Interestingly, in addition to Cu^{2+}, Fe^{2+}, and Zn^{2+}, Algp7 ($EfeO_{II}$) was found to be stabilized in the presence of the rare earth element (Sm^{3+}) by DSF (Fig. 2A), suggesting that Algp7 ($EfeO_{II}$) bound to Sm^{3+}.

To clarify the binding mode of Sm^{3+} toward Algp7 ($EfeO_{II}$), the crystal of Algp7 ($EfeO_{II}$) was prepared and soaked into the solution containing Sm^{3+} followed by X-ray crystallography. The resulting diffractions showed up to 1.88 Å resolution (Table S1). The resolution obtained herein (1.88 Å) is higher than that previously reported (1.99 Å, PDB ID: 3WSC) [9]. The whole structure is similar to that containing Cu^{2+} (Fig. 2B), however, there is no metal bound to Algp7 ($EfeO_{II}$). A citrate molecule formed two hydrogen bonds with Arg204 and Arg212. To clarify one of the reasons for no metal binding, the Algp7 ($EfeO_{II}$) structure determined in this

experiment was superimposed on that of Algp7 ($EfeO_{II}$) complexed with Cu^{2+} (PDB ID: 5Y4C) based on Cα. Among residues interacting directly with Cu^{2+}, Glu82 and Glu177 were oriented differently than those in the metal-unbound state (Fig. 2C). This suggested that Algp7 ($EfeO_{II}$) residues responsible for binding to metal ions lose their flexibility during crystallization and that samarium hardly bound to the Cu^{2+}-binding pocket.

3.4. X-ray crystallography of $EfeO_I$

Because structure of $EfeO_I$ remains to be determined, we attempted to express the strain A1 SPH728 ($EfeO_I$) in *E. coli* cells, but failed. Thus, $EfeO_I$ with a lack of signal peptide (Thr2-Ala26) from *E. coli* was expressed and purified in this study, because SPH728 ($EfeO_I$) exhibits a high sequence homology (identity, 41.7%, similarity, 56.9%) with *E. coli* $EfeO_I$. The residues in *E. coli* $EfeO_I$ are renumbered based on the lack of signal peptide. The X-ray crystal structure of *E. coli* $EfeO_I$ containing both cupredoxin and M75 peptidase domains at N- and C-terminus,

respectively, was determined at 1.85 Å resolution (Table S1, Fig. 3A left). This is the first structure of EfeO with both domains. Two domains were connected by a loop consisting of 4 residues. Although the primary structure of cupredoxin domain of $EfeO_I$ shows little similarity with those of other cupredoxin proteins (e.g. CupA), the tertiary structure of the domain formed Greek key β-barrel structure conserved among other cupredoxin proteins (Fig. 3A red). The database Interpro (https://www.ebi.ac.uk/interpro/) was used to find the same family proteins with cupredoxin domain of $EfeO_I$. As a result, 12 proteins were found as the same family. The tertiary structure of the cupredoxin domain of $EfeO_I$ was compared with CupA from *Streptococcus pneumoniae* (PDB ID: 4F2E) [20]. The identity of primary structure between two proteins was low, 14.4%. However, root mean square deviation (1.404 Å) of superimposed two proteins based on Cα showed similar structure (Fig. 3B). This result indicated that cupredoxin domain of $EfeO_I$ is involved in binding to cupper or electron transfer as seen in other CupA proteins. The M75 peptidase domain was composed of 10 α-helices as seen in other M75

peptidase domains (Fig. 3A yellow), and was structurally similar to Algp7 ($EfeO_{II}$) (Fig. 3C).

3.5 Structural insights into metal binding by $EfeO_I$

$EfeO_I$ has been suggested to have three metal-binding sites (I, II, and III) based on conservation of amino acid residues and tertiary structure built by homology modelling [5]. Site I (Cys16, Glu41, Met75, and Cys78) and site II (Glu43, Glu52, Glu53, and Glu55) located in the cupredoxin domain have also been predicted to bind to Cu^{2+} and Fe^{3+}, respectively. Site III (His192, x193, x194, and Glu 195) was in the M75 peptidase domain. Contrary to the predicted model, tertiary structure determined here revealed that four residues at the site I were structurally distant, and two Cys residues formed a disulfide bridge (Fig. 4A, green colored residues). At the site II, four residues also seemed to form incomplete metal-binding site because Glu52 faced opposite from the other residues (Fig. 4A, yellow colored residues). Multiple sequence alignment of cupredoxin proteins including EfeO indicated that Cys78 was

conserved and possibly involved in metal binding (Fig. 4B). Cys78 presumably binds to metals only in the reducing conditions and not in the oxidized conditions because of disulfide bridge formation. Metal binding at site I was considered to be regulated by redox balance in the periplasm.

The site III has been predicted to form zinc-binding motif "HxxE". However, three-dimensional arrangement of the four residues hardly formed tetrahedron geometry suitable for metal binding (Fig. 4C left, pink colored residues). Electron density map demonstrated that four other residues (Glu156, Glu159, Asp173, and Glu255) coordinated to a metal (Fig. 3A right). ICP-MS analysis revealed that most molecules (60%) of $EfeO_I$ possessed Zn^{2+}, indicating that Zn^{2+} was bound to these four residues. Because no zinc ion was added through the purification and crystallization steps, Zn^{2+} was probably bound to $EfeO_I$ in *E. coli* cells. The zinc-binding site in $EfeO_I$ completely corresponded to the copper-binding site of Algp7 ($EfeO_{II}$) (PDB ID: 5Y4C) (Fig. 4C right, blue colored residues). The four residues at the zinc-binding site are

highly conserved in EfeO proteins except for Pss1 (Fig. 4D). These results suggested that EfeO has a metal-binding site different from the HxxE motif (site III). This novel metal-binding site (Glu156, Glu159, Asp173, and Glu255) was proposed as "ExxE-//-D-//-E" motif.

In conclusion, this is the first report on crystal structure of EfeO with N-terminal cupredoxin and C-terminal M75 peptidase domains, and proposal of the novel metal-binding motif "ExxE-//-D-//-E" in EfeO C-terminal M75 peptidase domain.

Declaration of competing interest

The authors declare that they have no known competing financial interests or personal relationships that could have appeared to influence the work reported in this paper.

Acknowledgments

We thank Drs. S. Baba, N. Mizuno, G. Ueno, and H. Okumura for assistance with X-ray

data collection at the BL-26B1 and BL-38B1 beamlines in SPring-8 (Hyogo, Japan), which was approved by the Japanese Synchrotron Radiation Research Institute (Proposal Nos. 2017B2592, 2019A2557, 2020A2577, and 2021A2770). This work was supported in part by Grant-in-Aid for Scientific Research and Challenging Exploratory Research from the Japan Society for the Promotion of Science (W. H.) and by a research grant from The Toyo Suisan Foundation (W. H.). The authors would like to thank Enago (www.enago.com) for the English language review.

Appendix A. Supplementary data

Supplementary data to this article can be found online athttps://XXXXXXXXX.

References

[1] J A Morrissey, A Cockayne, P J Hill, P. Williams, Molecular cloning and analysis of a putative siderophore ABC transporter from *Staphylococcus aureus*, Infect. Immun. 68

(2000) 6281-6288.

[2] M L Cartron, S Maddocks, P Gillingham, C J Craven, S C Andrews, Feo-transport of ferrous iron into bacteria, Biometals 19 (2006), 143-157.

[3] J Cao, M R Woodhall, J Alvarez, M L Cartron, S C Andrews, EfeUOB (YcdNOB) is a tripartite, acid-induced and CpxAR-regulated, low-pH Fe^{2+} transporter that is cryptic in *Escherichia coli* K-12 but functional in *E. coli* O157:H7, Mol. Microbiol. 65 (2007) 857-875.

[4] X H Liu, Q Du, Z Wang, D Y Zhu, Y Huang, N Li, T D Wei, S J Xu, L C Gu, Crystal structure and biochemical features of EfeB/YcdB from *Escherichia coli* O157: ASP^{235} plays divergent roles in different enzyme-catalyzed processes, J. Biol. Chem. 286 (2011) 14922-14931.

[5] M B Rajasekaran, S Nilapwar, S C Andrews, K A Watson, EfeO-cupredoxins: major new members of the cupredoxin superfamily with roles in bacterial iron transport,

Biometals 23 (2010) 1-17.

[6] C Dennison, Investigating the structure and function of cupredoxins, Coordin. Chem. Rev. 249 (2005) 3025-3054.

[7] B Fricke, O Parchmann, K Kruse, P Rucknagel A Schierhorn, S Menge, Characterization and purification of an outer membrane metalloproteinase from *Pseudomonas aeruginosa* with fibrinogenolytic activity, Biochim. Biophys. Acta 1454 (1999) 236-250.

[8] J He, A Ochiai, Y Fukuda, W Hashimoto, K Murata, A putative lipoprotein of *Sphingomonas* sp. strain A1 binds alginate rather than a lipid moiety, FEMS Microbiol. Lett. 288 (2008) 221-226.

[9] K Temtrirath, K Murata, W Hashimoto, Structural insights into alginate binding by bacterial cell-surface protein, Carbohydr. Res. 404 (2015) 39-45.

[10] Y A Morch, I Donati, B L Strand, G Skjak-Braek, Effect of Ca^{2+}, Ba^{2+}, and Sr^{2+} on

alginate microbeads, Biomacromolecules 7 (2006) 1471-1480.

[11] Z Otwinowski, W Minor, Processing of X-ray diffraction data collected in oscillation mode, Methods Enzymol. 276 (1997) 307-326.

[12] W Kabsch, Xds, Acta Crystallogr. D Biol. Crystallogr. 66 (2010) 125-132.

[13] A Vagin, A Teplyakov, MOLREP: an automated program for molecular replacement, J. App. Crystallogr. 30 (1997) 1022-1025.

[14] P D Adams, P V Afonine, G Bunkoczi, V B Chen, I W Davis, N Echols, J Headd, L W Hung, G J Kapral, R W Grosse-Kunstleve, A J McCoy, N W Moriarty, R Oeffner, R J Read, D C Richardson, J S Richardson, T C Terwilliger, P H Zwart, PHENIX: a comprehensive Python-based system for macromolecular structure solution, Acta Crystallogr. D Biol. Crystallogr. 66 (2010) 213-221.

[15] G N Murshudov, A Vagin, E J Dodson, Refinement of macromolecular structures by the maximum-likelihood method, Acta Crystallogr. D Biol. Crystallogr. 53 (1997) 240-255.

[16] P Emsley, K Cowtan, Coot: model-building tools for molecular graphics, Acta Crystallogr. D Biol. Crystallogr. 60 (2004) 2126-2132.

[17] L C Schrodinger, The PyMOL molecular graphics system, version 1.3. (2010).

[18] K Temtrirath, K Okumura, Y Maruyama, B Mikami, K Murata, K, W Hashimoto, Binding mode of metal ions to the bacterial iron import protein EfeO. Biochem. Biophys. Res. Commun. 493 (2017) 1095-1101.

[19] M Saito, D Horiguchi, K Kina, Spectrophotometric determination of traces of iron(II) with novel water-soluble nitrosophenol derivatives. BUNSEKI KAGAKU 30 (1981) 525-1931.

[20] Y Fu, H T Tsui, K E Bruce, L Sham, K A Higgins, J P Lisher, K M Kazmierczak, M J Maroney, C E Dann, M E Winkler, D P Giedroc, A new structural paradigm in copper resistance in *Streptococcus pneumoniae*. Nat. Chem. Biol. 9 (2013) 177-183.

Figure legends

Fig. 1. EfeUOB cluster and structure/function of EfeB. (A) EfeUOB gene cluster in *Sphingomonas* sp. strain A1. *Cup* and *M75* represent cupredoxin and M75 peptidase domains, respectively. (B) Crystal structure of strain A1 EfeB (cyan) was determined through molecular replacement using the structure of *E. coli* EfeB (magenta) (PDB ID: 3O72). Green, blue, and red in the stick model represent carbon, nitrogen, and oxygen atoms in a heme molecule. (C) Heme-binding site in strain A1 EfeB. Green, cyan, blue, and red represent carbon in heme, carbon in EfeB, nitrogen, and oxygen atoms, respectively. Gray and cyan spheres show O_2 and water molecules, respectively. Dotted lines show hydrogen bonds. (D) Peroxidase activity of strain A1 EfeB in the presence or absence of reducing agents.

Fig. 2. Binding of rare earth element by and crystal structure of Algp7 ($EfeO_{II}$). (A) DSF analysis of Algp7 ($EfeO_{II}$) in the absence or presence of rare earth element (Sm^{3+}). The curves

show the negative derivative plot obtained from the fluorescence profile. Thermal shift to higher temperature was observed in the presence of the rare earth element (Sm^{3+}). (B) Structure of Algp7 ($EfeO_{II}$) was determined through molecular replacement using the previously clarified structure of Algp7 ($EfeO_{II}$) (PDB ID: 3AT7). Pink, Algp7 ($EfeO_{II}$) determined here; blue, Algp7 ($EfeO_{II}$) complexed with Cu^{2+} (PDB ID: 5Y4C). The right structure is rotated 90° toward the reader relative to that of left. (C) Copper-binding site in Algp7 ($EfeO_{II}$). Pink, carbon atoms of Algp7 ($EfeO_{II}$) determined here; blue, carbon atoms of Algp7 ($EfeO_{II}$) complexed with Cu^{2+} (PDB ID: 5Y4C).

Fig. 3. Crystal structure of $EfeO_I$. (A) Left, overall structure of *E. coli* $EfeO_I$. Red and yellow represent cupredoxin and M75 peptidase domains, respectively. Right, zinc bound (magenta) at the metal-binding site in the M75 peptidase domain of $EfeO_I$. Water molecules are colored blue. Glu159 and Glu255 are disordered. The *Phenix Polder* omit map for zinc and ligated residues

is shown with more than 3.5 σ. (B) Superimposition of the cupredoxin domain (red) of $EfeO_I$ and CupA (cyan). (C) Superimposition of the M75 peptidase domain (yellow) of $EfeO_I$ and Algp7 ($EfeO_{II}$) (blue). Zinc bound to $EfeO_I$ and copper bound to Algp7 ($EfeO_{II}$) are shown as magenta and green spheres, respectively.

Fig. 4. Structural alignment of metal-binding sites in EfeO. (A) Three-dimensional arrangement of site I (green) and II (yellow) residues in the cupredoxin domain (red) of $EfeO_I$. (B) Multiple sequence alignment of the $EfeO_I$ cupredoxin domain and other cupredoxin proteins. The residue numberings for $EfeO_I$ are shown at the top. Site I (green), site II (yellow), copper binding site (cyan) residues. (C) Left, close-up site III (left, magenta colored) in $EfeO_I$. Right, close-up metal-binding site in the M75 peptidase domain of $EfeO_I$ (yellow) and Algp7 ($EfeO_{II}$) (blue). Zinc bound to $EfeO_I$ and copper bound to Algp7 ($EfeO_{II}$) are shown as magenta and green spheres, respectively. (D) Multiple sequence alignment of M75 peptidase domain proteins

(orange, $EfeO_I$; cyan, $EfeO_{II}$). The residue numberings for $EfeO_I$ are shown at the top. Site III (magenta), metal-binding site residues (blue).

1 Figure 1

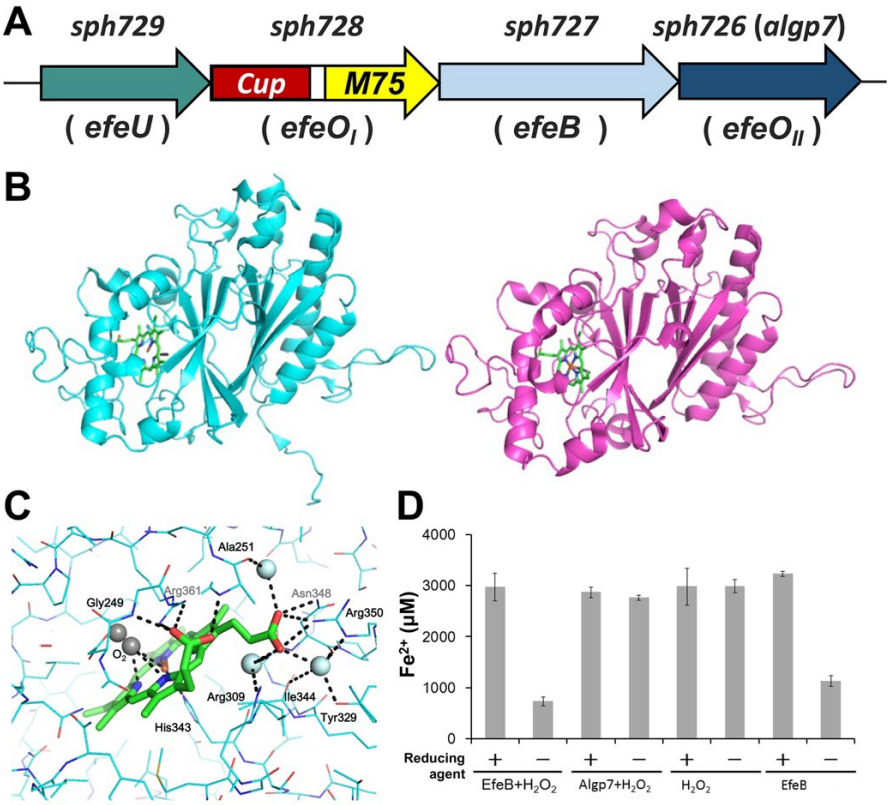
A
sph729
sph728
sph727
sph726 (algp7)
Cup
M75
(efeU)
(efeO$_I$)
(efeB)
(efeO$_{II}$)
B
C
Ala251
Arg361
Asn348
Gly249
Arg350
O$_2$
Arg309
Ile344
Tyr329
His343
D
Fe^{2+} (μM)
4000
3000
2000
1000
0
Reducing agent
+ − + − + − + −
EfeB+H$_2$O$_2$
Algp7+H$_2$O$_2$
H$_2$O$_2$
EfeB

2

3

Figure 2

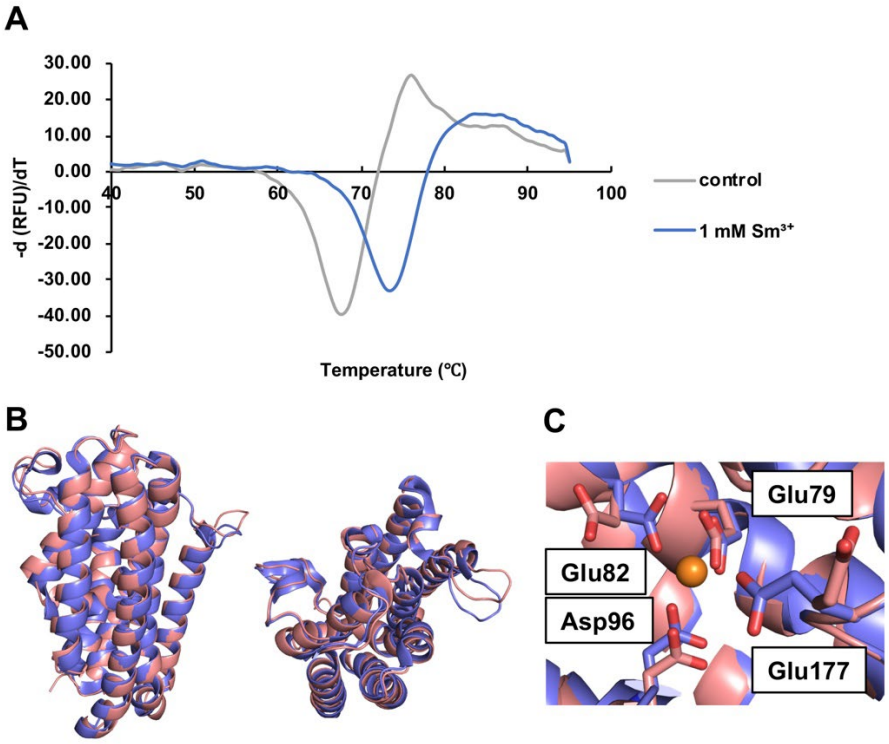
A
30.00
20.00
10.00
0.00
-10.00
-20.00
-30.00
-40.00
-50.00
-d (RFU)/dT
40
50
60
70
80
90
100
Temperature (℃)
control
1 mM Sm3+
B
C
Glu79
Glu82
Asp96
Glu177

Figure 3

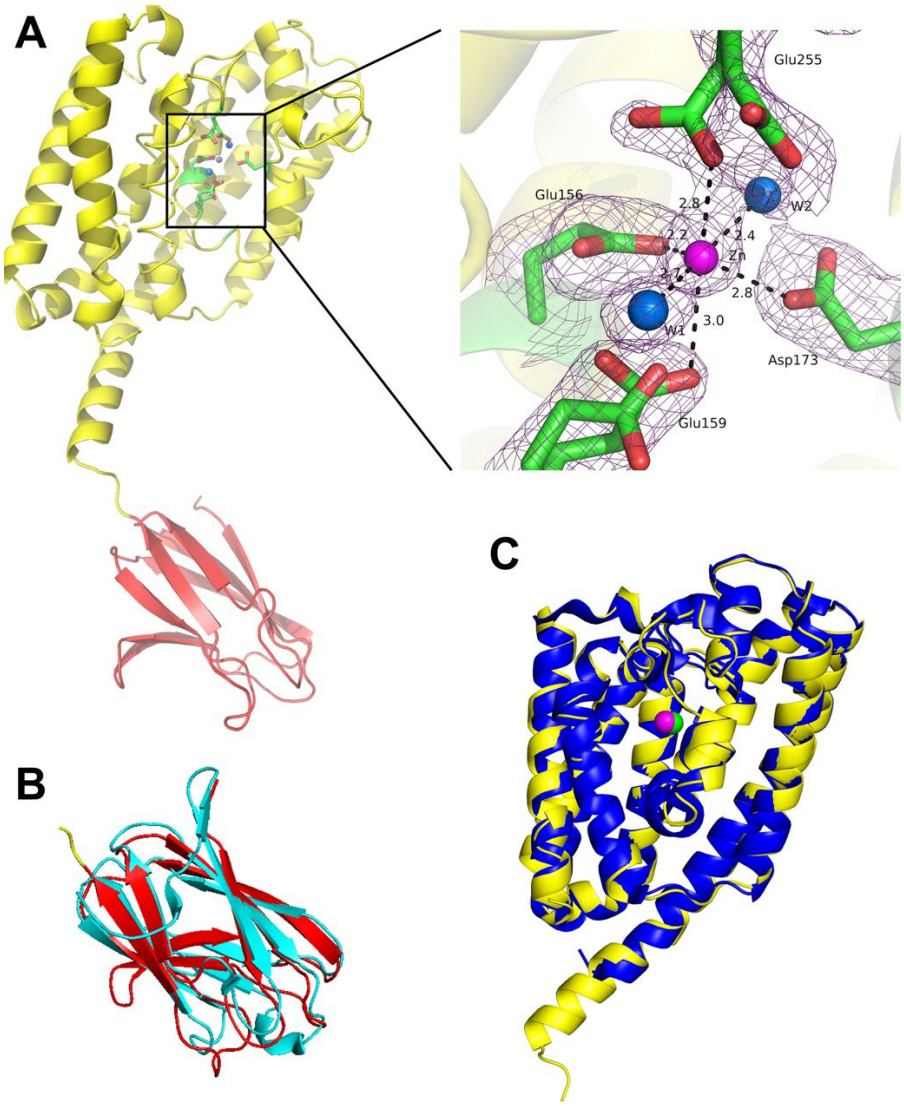

Figure 4

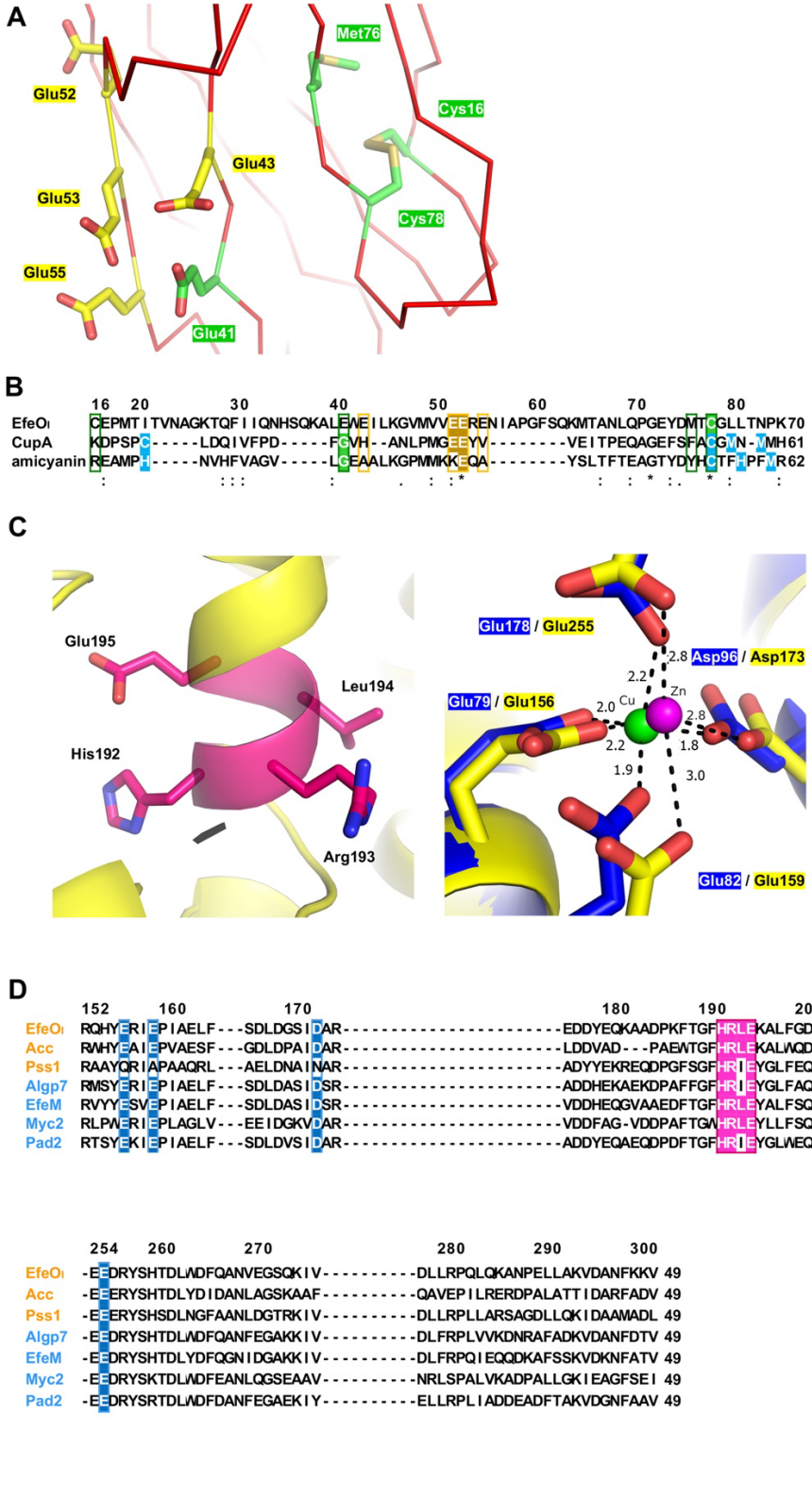
A
Met76
Glu52
Cys16
Glu43
Glu53
Cys78
Glu55
Glu41
B
16 20 30 40 50 60 70 80
EfeO1 CEPMTITVNAGKTQFIIQNHSQKALEVEILKGVMVVEERENIAPGFSQKMTANLQPGEYDMTCGLLTNPK 70
CupA KDPSPC-----LDQIVFPD-----FGVH--ANLPMGEEYV--------VEITPEQAGEFSFACGVN-VMH 61
amicyanin REAMPH-----NVHFVAGV-----LGEAALKGPMMKKEQA--------YSLTFTEAGTYDYHCTFHPFMR 62
C
Glu195
Leu194
His192
Arg193
Glu178 / Glu255
Asp96 / Asp173
Glu79 / Glu156
Cu
Zn
2.8
2.2
2.0
2.8
2.2
1.8
1.9
3.0
Glu82 / Glu159
D
152 160 170 180 190 200
EfeO1 RQHYERIEPIAELF---SDLDGSIDAR----------EDDYEQKAADPKFTGFHRLEKALFGDN 51
Acc RWHYEAIEPVAESF---GDLDPAIDAR----------LDDVAD---PAEWTGFHRLEKALWQDD 48
Pss1 RAAYQRIAPAAQRL---AELDNAINAR----------ADYYEKREQDPGFSGFHRIEYGLFEQH 51
Algp7 RMSYERIEPIAELF---SDLDASIDSR----------ADDHEKAEKDPAFFGFHRIEYGLFAQN 51
EfeM RVYYESVEPIAELF---SDLDASIDSR----------VDDHEQGVAAEDFTGFHRLEYALFSQN 51
Myc2 RLPAERIEPLAGLV---EEIDGKVDAR----------VDDFAG-VDDPAFTGWHRLEYLLFSQN 50
Pad2 RTSYEKIEPIAELF---SDLDVSIDAR----------ADDYEQAEQDPDFTGFHRIEYGLWEQG 51
254 260 270 280 290 300
EfeO1 -EEDRYSHTDLWDFQANVEGSQKIV----------DLLRPQLQKANPELLAKVDANFKKV 49
Acc -EEERYSHTDLYDIDANLAGSKAAF----------QAVEPILRERDPALATTIDARFADV 49
Pss1 -EEERYSHSDLNGFAANLDGTRKIV----------DLLRPLLARSAGDLLQKIDAAMADL 49
Algp7 -EEDRYSHTDLWDFQANFEGAKKIV----------DLFRPLVVKDNRAFADKVDANFDTV 49
EfeM -EEDRYSHTDLYDFQGNIDGAKKIV----------DLFRPQIEQQDKAFSSKVDKNFATV 49
Myc2 -EEDRYSKTDLWDFEANLQGSEAAV----------NRLSPALVKADPALLGKIEAGFSEI 49
Pad2 -EEDRYSRTDLWDFDANFEGAEKIY----------ELLRPLIADDEADFTAKVDGNFAAV 49

Table S1. X-ray data collection and structure refinement statistics.

	EfeB	Algp7 ($EfeO_{II}$)	$EfeO_I$
Data collection			
Wavelength (Å)	1.0000	1.0000	1.0000
Space group	$P2_12_12_1$	$P2_12_12_1$	$C2$
Unit cell parameters (Å, °)	a = 100.0, b = 105.0, c = 83.8	a = 52.8, b = 97.5, c = 104.9	a = 139.9, b = 51.9, c = 117.4 α= 90.0, β = 112.4, γ = 90.0
Resolution limit (Å)	50.0 – 2.30 (2.44 – 2.30)[a]	50.0 – 1.88 (1.91 – 1.88)[a]	50.0 – 1.85 (1.96 – 1.85)[a]
Total reflections	307,536 (50,278)[a]	307,493 (14,878)[a]	249,772 (33,933)[a]
Unique reflections	38,892 (6,217)[a]	44,838 (2,188)[a]	65,646 (9,994)[a]
Completeness (%)	97.5 (97.9)[a]	99.8 (99.3)[a]	97.7 (92.8)[a]
I/σ (I)	19.4 (10.2)[a]	36.5 (5.3)[a]	18.5 (2.48)[a]
R_{merge} (%)	6.1 (14.8)[a]	7.2 (48.3)[a]	3.9 (40.0)[a]
CC(1/2)	99.9 (99.7)[a]	99.9 (95.7)[a]	99.9 (91.8)
Wilson B ($Å^2$)	31.2	28.0	37.9
Refinement			
Resolution limit (Å)	44.5 – 2.30 (2.36 – 2.30)[a]	46.5 – 1.88 (1.92 – 1.88)[a]	48.2 – 1.85 (1.87 – 1.85)[a]
R-factor (%)	23.4 (24.8)[a]	18.2 (25.1)[a]	20.1 (34.0)[a]
R_{free} (%)	29.8 (36.0)[a]	21.8 (33.0)[a]	24.4 (37.3)[a]
Final model	781 residues, 257 waters, 24 1,2-ethanediol, 1 oxygen molecule, 5 di (hydroxyethyl) ether, 3 triethylene glycol, 2 heme	502 residues, 421 waters, 9 1,2-ethanediol, 1 citrate	697 residues, 322 waters, 30 1,2-ethanediol, 1 acetate, 1 sulfate, 1 triethylene glycol, 1 zinc ion
r.m.s.d.			
Bond (Å)	0.008	0.01	0.006
Angle (°)	0.971	1.47	0.806
Ramachandran plot (%)			
Favored regions	96.0	98.0	98.1
Allowed regions	3.5	1.8	1.7
Outliers	0.5	0.2	0.14
Clashscore	7	8	5.85
Rotamer ouliers (%)	0.63	0	2.5
PDB ID	6JBN	6JBO	7WGU

[a] Data on highest shells are given in parenthesis.